Perineuronal nets protect fast-spiking interneurons against oxidative stress

Jan-Harry Cabungcal[a,1], Pascal Steullet[a,1], Hirofumi Morishita[b,2], Rudolf Kraftsik[c], Michel Cuenod[a], Takao K. Hensch[b,d], and Kim Q. Do[a,3]

[a]Center for Psychiatric Neuroscience, Department of Psychiatry, Centre Hospitalier Universitaire Vaudois and University of Lausanne, 1008 Prilly-Lausanne, Switzerland; [c]Department of Fundamental Neuroscience, University of Lausanne, 1005 Lausanne, Switzerland; [b]F. M. Kirby Neurobiology Center, Boston Children's Hospital, Harvard Medical School, Boston, MA 02115; and [d]Center for Brain Science, Department of Molecular Cellular Biology, Harvard University, Cambridge, MA 02138

A hallmark of schizophrenia pathophysiology is the dysfunction of cortical inhibitory GABA neurons expressing parvalbumin, which are essential for coordinating neuronal synchrony during various sensory and cognitive tasks. The high metabolic requirements of these fast-spiking cells may render them susceptible to redox dysregulation and oxidative stress. Using mice carrying a genetic redox imbalance, we demonstrate that extracellular perineuronal nets, which constitute a specialized polyanionic matrix enwrapping most of these interneurons as they mature, play a critical role in the protection against oxidative stress. These nets limit the effect of genetically impaired antioxidant systems and/or excessive reactive oxygen species produced by severe environmental insults. We observe an inverse relationship between the robustness of the perineuronal nets around parvalbumin cells and the degree of intracellular oxidative stress they display. Enzymatic degradation of the perineuronal nets renders mature parvalbumin cells and fast rhythmic neuronal synchrony more susceptible to oxidative stress. In parallel, parvalbumin cells enwrapped with mature perineuronal nets are better protected than immature parvalbumin cells surrounded by less-condensed perineuronal nets. Although the perineuronal nets act as a protective shield, they are also themselves sensitive to excess oxidative stress. The protection might therefore reflect a balance between the oxidative burden on perineuronal net degradation and the capacity of the system to maintain the nets. Abnormal perineuronal nets, as observed in the postmortem patient brain, may thus underlie the vulnerability and functional impairment of pivotal inhibitory circuits in schizophrenia.

critical period | extracellular matrix | glutamate cysteine ligase | glutathione | neuronal synchronization

Fast-spiking interneurons expressing parvalbumin (PV) constitute a subpopulation of GABA cells that control the output of principal neurons and are necessary for fast rhythmic neuronal synchrony, facilitating information processing during cognitive tasks (1, 2). To coordinate the activity of neuronal assemblies, PV cells are interconnected by both chemical and electrical synapses, have the capacity to fire at high frequency without adaptation, and selectively position inhibitory synaptic terminals onto the cell body and axon initial segment of their target neurons. Fast-spiking properties consequently impose high metabolic demand and increased mitochondrial density, which renders PV cells, but not other interneurons such as calretinin and calbindin cells, particularly sensitive to oxidative stress (3). For instance, ketamine induces superoxide overproduction that strongly impairs PV cells (i.e., loss of normal phenotype including PV immunoreactivity but without cell death) (4, 5). Moreover, severe environmental stressors produce oxidative stress in the brain and impair PV cells (6–8). Postmortem studies reveal PV-cell anomalies in individuals with schizophrenia or bipolar disorder (9–11). Abnormal neuronal synchrony in γ-frequency (30–80 Hz) and β-frequency (13–28 Hz) bands during sensory and cognitive processing tasks (12–15)

further indicates a PV cell network dysfunction in schizophrenia. Parallel evidence of oxidative stress and altered antioxidant response is also found both in schizophrenia and in bipolar disorder (16, 17). Oxidative stress and decreased levels of the endogenous antioxidant and redox regulator glutathione (GSH) are observed in the prefrontal cortex of patients (18–20). Therefore, redox dysregulation via impaired GSH synthesis (21, 22) or abnormal function of proteins encoded by other susceptibility genes [i.e., proline dehydrogenase (oxidase) 1 (*PRODH*), disrupted in schizophrenia 1 (*DISC1*), D-amino acid oxidase activator (*DAOA* or *G72*), dystrobrevin binding protein 1 (*DTNBP1*)] (23–27) could, together with oxidative stress generated by environmental insults, contribute to the pathophysiology of these disorders (28, 29).

Here, we explore whether these metabolically intense interneurons have evolved unique protective mechanisms to limit their intrinsic vulnerability. When most fast-spiking PV cells mature (30), they become enwrapped by a specialized extracellular matrix or aggrecan-enriched perineuronal nets (PNNs). These PNNs consist of highly charged chondroitin sulfate proteoglycans (e.g., aggrecan, neurocan, brevican), hyaluronan, tenascin, and link proteins (31). The PNNs promote interneuron maturation and synaptic and network stability (reviewed in refs. 32 and 33). It has also been suggested that PNNs may protect neurons against iron sequestration and oxidative stress (34, 35). Therefore, we examined the relationship between the PNNs around PV cells and oxidative stress in mice that suffer from a genetic redox dysregulation and that are consequently more susceptible to oxidative stress. These mice do not express the modulatory subunit of the glutamate cysteine ligase (*Gclm*, ref. 36), the rate-limiting enzyme of GSH synthesis. These *Gclm* knockout (KO) mice have low brain GSH levels (∼30% of WT levels) (37) and represent a valid animal model, as low brain GSH levels (18, 19) and genetic association with *GCLM* have been reported in schizophrenia (22). We assessed both the cumulative effect of chronic redox dysregulation and the effect of additional oxidative challenges applied at different ages. The anterior cingulate cortex (ACC) was chosen as a prefrontal area known to be affected and to display redox dysregulation in schizophrenia (20). In this study, we provide experimental evidence that the PNNs protect mature PV cells against oxidative stress.

Results

Six-Month Chronic Redox Dysregulation Preferentially Affects PV Cells Lacking PNNs. Compared with WT mice, the ACC of young adult (postnatal day, P90) *Gclm* KO mice displayed significantly more oxidative stress, as revealed by the presence of 8-oxo-7,8-dihydro-20-deoxyguanine (8-oxo-dG), a product of DNA oxidation [8-oxo-dG intensity (arbitrary unit, mean ± SD): 2.16 ± 0.18 (KO) vs. 1.12 ± 0.66 (WT); 4 mice each; P = 0.02]. This level of oxidative stress was, however, insufficient to significantly affect PV cells [number of PV immunoreactive cells: 71.8 ± 12.6 (KO) vs. 71.3 ± 12.8 (WT)] or PNNs labeled with the lectin *Wisteria floribunda* agglutinin (WFA). A large population of WFA-positive PNNs is associated with PV cells (38). The number of PV cells with WFA-labeled PNNs [54.8 ± 7.5 (KO) vs. 52.8 ± 9.2 (WT)] and the overall intensity of WFA labeling [arbitrary unit: 2.9 ± 0.2 (KO) vs. 3.0 ± 0.9 (WT)] were not significantly different between genotypes.

However, as *Gclm* KO mice aged further, the chronic deficit in GSH eventually led to PV-cell impairment. Although the oxidative stress levels were similar in P90 and P180 *Gclm* KO mice, the ACC of P180 *Gclm* KO mice contained fewer PV immunoreactive cells (Fig. 1 *A* and *B*) compared with age-matched WT mice. In contrast, WFA-labeled PNNs were not affected (Fig. 1 *A* and *B*). The proportion of PV cells surrounded by PNNs was consequently higher in P180 *Gclm* KO mice than in age-matched WT mice (Fig. 1 *A* and *B*). This led us to hypothesize that PV cells enwrapped by well-formed PNNs may have been better protected against a 6-mo chronic oxidative stress. As PV cells are involved in fast rhythmic neuronal synchrony, we assessed whether the decreased number of PV immunoreactive cells was associated with altered local neuronal synchrony in P180 *Gclm* KO mice. Fast oscillatory neuronal activity was induced in ACC slices by coapplication of carbachol, kainic acid, and quinpirole (Fig. S1). Power spectrum analysis of the extracellular recordings revealed prominent β oscillations (13–28 Hz)

accompanied by smaller γ oscillations (30–60 Hz), reflecting rhythmic neuronal synchronization at these frequencies (Fig. S1). In the ACC of P90 mice that showed no deficit in the number of PV immunoreactive cells, these oscillations were not significantly different between genotypes (Fig. S2). In contrast, the ACC of P180 *Gclm* KO mice, which contained fewer PV immunoreactive cells (Fig. 1*B*), displayed significantly weaker β and γ oscillations compared with the ACC of age-matched WT mice (Fig. 1 *C* and *D*). Taken together, accumulated oxidative stress resulting from a very long chronic redox dysregulation (as in P180 mice but not P90 mice) impairs many PV cells and their associated local neuronal synchrony while sparing those PV cells bearing well-formed PNNs.

Immature PV Cells Bearing Less-Condensed PNNs Are More Vulnerable to Oxidative Stress. If mature WFA-labeled PNNs are protective, one would expect PV cells to be highly sensitive to oxidative stress in younger animals, when these PNNs are not yet well-formed. In P20 *Gclm* KO mice, the WFA-labeled PNNs had not yet fully condensed compared with those at P90 (Fig. 2*A*). We compared the effects of an additional pharmacological stressor on PV cells across these ages. *Gclm* KO mice were injected daily with a specific dopamine reuptake inhibitor, 1-[2-[*Bis*-(4-fluorophenyl)methoxy]ethyl]-4-(3-phenylpropyl)piperazine dihydrochloride (GBR12909, GBR), either from P10 to P20 or from P80 to P90. GBR increases extracellular dopamine, which in turn generates reactive oxygen species (ROS) (39, 40) in regions richly innervated by dopaminergic terminals, such as the ACC. This pharmacological approach partially mimics the pronounced prefrontal dopamine release during psychosocial stress (41, 42).

GBR induced a significant increase of 8-oxo-dG signal in the entire ACC of *Gclm* KO mice at both ages (P20 and P90), but the labeling was significantly higher at P20 (Fig. 2*C*). GBR-induced oxidative stress was accompanied by a decreased number of PV immunoreactive cells at P20, but not at P90 (Fig. 2*B*). In contrast, GBR-generated ROS were not sufficient to elicit oxidative stress in WT mice with an intact antioxidant system (Fig. S3). Because GBR neither significantly induced 8-oxo-dG labeling nor altered PV immunoreactivity in WT mice at either age (Fig. S3), this indicates that PV-cell impairment in preweaning GBR-treated KO mice was associated with the induced oxidative stress and not with other dopamine-mediated mechanisms. Furthermore, the antioxidant *N*-acetylcysteine prevents the GBR-induced PV-cell defect in *Gclm* KO mice (3). Taken together, these data suggest that fully mature WFA-labeled PNNs (as seen in P90 *Gclm* KO mice) are able to limit the GBR-induced increase in oxidative stress throughout the ACC, and therefore prevent PV-cell impairment at this age.

We further quantified the correspondence of PNN robustness and oxidative stress in PV cells. The amount of WFA-labeled PNNs and 8-oxo-dG signal associated with individual PV cells in the ACC of P90 *Gclm* KO mice following GBR treatment were conjointly plotted. The degree of oxidative stress per PV cell (8-oxo-dG labeling) varied with the PNN density (WFA labeling) surrounding it, yielding a significant inverse correlation (Fig. 2*D*). Thus, PV cells enwrapped by well-formed PNNs displayed less oxidative stress.

PNNs Are Themselves Sensitive to Excessive Redox Dysregulation. Although the additional oxidative stress generated by GBR did not affect PV immunoreactivity in P90 *Gclm* KO mice (Fig. 2*B*), it led to an overall decrease in WFA labeling around PV cells (Fig. 3). This indicates that although PNNs limit oxidative stress and protect PV cells, they are also by themselves sensitive to excess amounts of oxidative stress. We then investigated the effects of a cell-autonomous redox dysregulation on PV immunoreactivity and WFA-labeled PNNs. We generated mice whose PV cells were fully incapable of synthesizing GSH by a restricted

Fig. 1. Chronic 6-mo redox dysregulation preferentially affects PV cells lacking PNNs. (*A*) PV immunoreactivity (red) and WFA-labeled PNNs (green) in the ACC of adult (P180) *Gclm* KO and WT mice. (Scale, 40 μm.) (*B*) (*Left*) stereological quantification reveals fewer PV immunoreactive cells in KO mice than in WT mice (n = 6 per group). (*Center*) WFA-labeled PNNs are not affected in KO mice. (*Right*) percentage of PV immunoreactive cells enwrapped by WFA-labeled PNNs is higher in KO mice, suggesting that the affected PV cells were those lacking PNNs. (*C*) Local neuronal synchronization in ACC slices (induced by carbachol, kainic acid, and quinpirole) is reduced in P180 KO mice. The power of β- (13–28 Hz; *Left*) and γ-oscillations (30–60 Hz; *Right*) is weaker in KO (n = 11) vs. WT slices (n = 15). (*D*) Power spectra of KO and WT recordings (mean of pooled data). Note that the peak frequencies of both β and γ oscillations do not differ significantly across genotypes [mean ± SD; β peak: 21.8 ± 3.2 Hz (KO) and 21.0 ± 2.3 Hz (WT); γ peak: 40.8 ± 5.6 Hz (KO) and 41.0 ± 4.5 Hz (WT)]. Bars, SD. **P < 0.01; *P < 0.05.

NEUROSCIENCE

Fig. 2. Mature PNNs protect PV cells from oxidative stress. (A) WFA-labeled PNNs in P20 *Gclm* KO mice are not fully developed around PV cells compared with P90 mice (*n* = 5 per group). Micrographs of PV immunoreactivity (red) and WFA labeling (green) in the ACC. (Scale, 40 μm.) (B) GBR-induced oxidative stress only affects PV cells in P20 *Gclm* KO. Micrographs of PV immunoreactivity in the ACC of P20 GBR- and PBS-treated KO mice. (Scale, 80 μm.) (C) GBR treatment generates significant additional oxidative stress in the ACC of P20 and P90 *Gclm* KO mice (*n* = 4 per group). Micrographs of 8-oxo-dG labeling after GBR treatment. (Scale, 40 μm.) (D) PV cells (red or arrowheads) surrounded by dense WFA-labeled PNNs (light blue, pseudo-color modified for improved visibility) display low levels of 8-oxo-dG signal (green), and vice versa. (Scale, 10 μm.) Quantile density contours and linear regression plot illustrate the inverse relationship between the number of voxels stained with WFA (PNNs) and 8-oxo-dG associated with each PV cell. Rank-transformed values for WFA (rWFA) and 8-oxo-dG (r8-oxo-dG) were used to compute the Pearson correlation coefficient. Bars, SD. **$P < 0.01$; *$P < 0.05$.

deletion of the gene coding for the catalytic subunit of glutamate cysteine ligase (GCLC), only in PV cells. *PV-Gclc* KO mice showed a progressive GCLC deletion in PV-expressing cells, with ~70% of PV-Cre(+) cells displaying no *Gclc* mRNA in the cerebral cortex of 2-mo-old animals. These conditional KO mice displayed a much stronger 8-oxo-dG labeling within PV cells compared with *PV-Gclc* WT mice (Fig. 4 *A* and *B*) or *Gclm* KO mice (Fig. S4). Under such severe cell-autonomous redox dysregulation, significantly fewer PV immunoreactive cells and WFA-labeled PNNs were observed (Fig. 4 *C* and *D*). In cortical layers enriched in PV cells, some cells displayed strong 8-oxo-dG labeling, although they were neither PV immunoreactive (Fig. 4*A*) nor enwrapped by WFA-labeled PNNs. These may represent PV cells that had already lost PV immunoreactivity. However, in this model, it remains unclear whether the loss of WFA-labeled PNNs precedes the loss of PV expression or whether it is the consequence of PV-cell dysfunction or degeneration.

Degradation of Mature PNNs Renders PV Cells More Susceptible to Oxidative Stress.

To substantiate whether mature PNNs play a protective role, we stripped them off the ACC of young adult (P90) *Gclm* KO mice and monitored PV-cell susceptibility to oxidative stress, using GBR. The chondroitinase ABC (ChABC) enzyme was locally injected into one ACC, and the contralateral side received a vehicle (sham). ChABC injection efficiently degraded PNNs unilaterally, as verified 2 d postinjection by the absence of WFA labeling in the treated ACC (Fig. S5). After ChABC injection, mice were further treated for 11 consecutive days with either GBR or a vehicle (PBS) and then killed (Fig. 5*D*). In both PBS-treated (*n* = 5) and GBR-treated (*n* = 7) mice, WFA labeling in the ChABC-injected ACC was faint and significantly weaker than in sham ACC (*P* < 0.001; Fig. 5*A*). However, only GBR caused a significant decrease in the number of PV immunoreactive cells in the ChABC-injected ACC compared with the contralateral side (Fig. 5*B*). The 8-oxo-dG labeling after GBR treatment was likewise significantly higher in ChABC-injected than in sham ACC (Fig. 5*C*). PNN degradation did not, however, affect the number of calbindin- and calretinin-immunoreactive cells when subjected to GBR-induced oxidative stress (Fig. S6). This demonstrates that mature PNNs specifically protect PV cells from additional oxidative stress.

Finally, we functionally assessed whether PNN degradation rendered local PV-cell networks vulnerable to further oxidative stress. Fast rhythmic oscillations reflecting neuronal synchronization were clearly altered in slices of ChABC-injected ACC from the P90 GBR-treated *Gclm* KO mice [significant interaction between treatment (PBS vs. GBR) and PNN status (ChABC vs. contralateral sham), multivariate analysis; *P* = 0.039]. In control PBS-treated *Gclm* KO mice, the power of oscillations (induced by coapplication of carbachol, kainic acid, and quinpirole) tended to be stronger in the ChABC-injected side compared with contralateral sham ACC (Fig. 5*E*). Instead, in GBR-treated *Gclm* KO mice, the power of oscillations tended to be weaker in the ChABC-injected side compared with sham ACC (Fig. 5*F*). Thus, a lack of PNNs favors β/γ oscillatory power, which is then weakened during oxidative stress challenge, consistent with the reduced number of PV immunoreactive cells under the latter condition (Fig. 5*B*).

Discussion

Our study provides experimental evidence that intact and mature WFA-labeled PNNs protect fast-spiking PV cells against oxidative stress. This can explain our observation that PV cells enwrapped with well-formed WFA-labeled PNNs, but not PV cells lacking WFA-labeled PNNs, are protected against a long-lasting chronic redox dysregulation (as in P180 *Gclm* KO mice).

Fig. 3. PNNs are sensitive to additional oxidative stress in *Gclm* KO mice. (A) Micrographs of PV (red) and WFA labeling (green) after GBR treatment in P90 *Gclm* KO and WT mice. (Scale, 40 μm.) (B) Quantification (*n* = 5 per group) shows that the number of PV immunoreactive cells is not significantly different in GBR-treated WT and KO mice (*Left*). However, GBR significantly reduces WFA labeling in KO compared with WT mice (*Right*). Bars, SD. ***$P < 0.001$.

Fig. 4. PV cells and their PNNs are sensitive to cell-autonomous redox dysregulation. (*A*) Redox dysregulation restricted to PV cells (PV-*Gclc* KO mice) leads to strong 8-oxo-dG signals within PV cells of the ACC. Some cells without PV but with strong 8-oxo-dG labeling may have lost their PV immunoreactivity. (Scale, 10 μm.) (*B*) Quantification shows higher 8-oxo-dG labeling within the ACC (*Left*) and within PV cells (percentage PV colocalized with 8-oxo-dG; *Right*) of PV-*Gclc* KO compared with PV-*Gclc* WT mice (*n* = 5 per group). (*C*) PV immunoreactivity and WFA-labeled PNNs in the ACC of PV-*Gclc* KO and WT mice. (Scale, 50 μm.) (*D*) Quantification indicates significant decrease in number of PV immunoreactive cells (*Left*) and PNNs (*Right*) in PV-*Gclc* KO mice (*n* = 5 per group). Bars, SD. ***P < 0.001; **P < 0.01.

The higher susceptibility of PV cells to oxidative stress (this study) and to ROS (5) in preweaning compared with adult mice might also be related to the lack of fully condensed PNNs around immature PV cells. However, we cannot exclude the possibility that other additional factors might contribute to the high vulnerability of these cells during their maturation.

Our work provides experimental support to observations suggesting that PNNs are neuroprotective (34, 35). Through their poly-anionic nature, PNNs chelate iron (43), thereby limiting the formation of iron-generated reactive hydrogen radicals. Components of the PNNs, such as hyaluronan and chondroitin sulfate, have antioxidant properties (44, 45) and can reduce the generation of hydroxyl radical (OH) via their capacity to chelate transition metals and limit the initiation of Harber-Weiss and Fenton's reactions. This, in turn, decreases lipid peroxidation, DNA damage, and protein oxidation. Notably, PNN degradation by ChABC exacerbated the GBR-induced increase of 8-oxo-dG labeling throughout the ACC, not just in PV cells (Fig. 5*C*).

Chondroitin sulfate has further been shown to decrease the production of ROS generated by H_2O_2 or mitochondrial disruption by induction of the antioxidant enzyme heme oxygenase-1 through the phosphatidylinositol 3-kinase (PI3K)/protein kinase B (Akt) pathway (45). Thus, intact PNNs could serve as a protective shield to neutralize ROS either directly and/or via activation of intracellular pathways to boost the cellular antioxidant capacity. Selenoprotein deficiency likewise reduces the number of PV cells and impairs behaviors such as fear learning and sensorimotor gating in mice (46). Conversely, we also show that WFA-labeled PNNs themselves suffer from excessive oxidative stress or severe redox dysregulation.

ROS is known to break down two PNN components, hyaluronan and chondroitin sulfate (47). Traumatic injury, which causes a rapid and strong increase in superoxide production and oxidative stress (48), notably leads to a transient reduction of WFA-labeled PNNs rendering the damaged tissue permissive for axon sprouting (49).

In addition to reduced PV expression and abnormal expression of several pre- and postsynaptic markers associated with PV cells, a significant decrease in WFA-labeled PNNs has recently been reported in patients with schizophrenia (50), potentially reflecting oxidative stress and decreased levels of GSH. However, PNN anomalies could also have other origins. Pantazopoulos
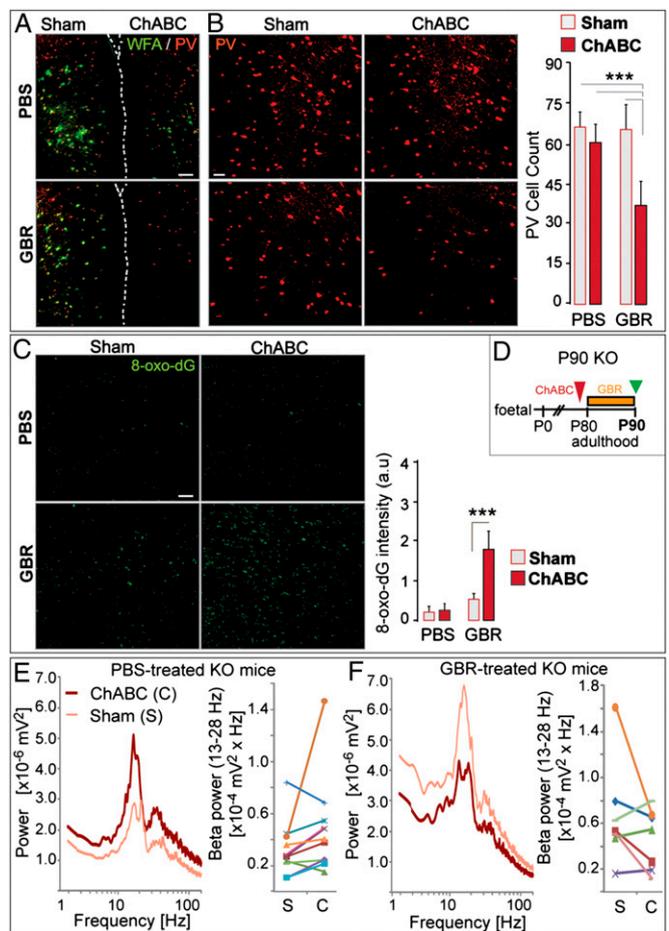
Fig. 5. PNN removal by ChABC renders PV cells vulnerable to oxidative stress. (*A*) WFA (green) and PV (red) labeling after GBR or PBS treatment in ChABC-injected and contralateral sham ACC of P90 *Gclm* KO mice. Dashed line: separation of hemispheres (ChABC-injected ACC; *Right*). (Scale, 100 μm.) (*B*) GBR (*n* = 7), but not PBS (*n* = 5), induces a significant decrease in PV immunoreactive cells in ChABC-injected ACC. (Scale, 50 μm.) (*C*) The 8-oxo-dG labeling in ChABC-injected and contralateral sham ACC after GBR or PBS treatment. (Scale, 80 μm.) The 8-oxo-dG signal is stronger in ChABC-injected ACC after GBR treatment. (*D*) Experimental design. (*E* and *F*) Neuronal synchronization induced by coapplication of carbachol, kainic acid and quinpirole in PBS- (*n* = 5) (*E*) and GBR-treated (*n* = 5) (*F*) KO mice. The effect of PNN degradation on the oscillation power depends on the treatment (PBS vs. GBR): significant interaction (P = 0.039, multivariate analysis) between PNN status in ACC (ChABC- vs. sham-injected) and treatment (PBS vs. GBR). In PBS-treated mice, oscillations tend to be higher in ChABC-injected compared with contralateral sham ACC (9 of 11 slices) (*E*). In contrast, in GBR-treated mice, oscillations tend to be weaker in ChABC-injected compared with contralateral sham ACC (4 of 7 slices) (*F*). Graphs indicate the paired power values recorded in a ChABC-injected ACC and its contralateral sham ACC connected by a line. Bars, SD. ***P < 0.001.

et al. (50) reported that the reduction of WFA-labeled PNNs is accompanied by an increase of chondroitin sulfate proteoglycans within glial cells of patients with schizophrenia, suggesting a defect in the capacity of glial cells to excrete some of the PNN components. Moreover, a genetic association has been found between schizophrenia and the gene B3GAT2, which is involved in biosynthesis of the human natural killer-1 (HNK-1) carbohydrate epitope of tenascin, a major constituent of PNNs (51).

PV cell protection might then reflect a balance between the oxidative burden on PNN degradation and the capacity of PV cells and nearby glial or neuronal cells to maintain the extracellular nets. Importantly, PNNs control the accumulation of a noncell autonomous homeoprotein, orthodenticle homeobox 2 (Otx2), within PV cells. Both specific interactions with sugar residues in the PNNs (52) or sulfation patterns (53) enable the persistent uptake of this factor, which in turn promotes PNN formation, suggesting a positive feedback loop for PV-cell maintenance. Across multiple neuropsychiatric disorders, including autism, schizophrenia, and bipolar disorder, the developmental gene expression program in PV cells is instead immature (54). Our data are thus directly relevant to the anomalies of PV-cell networks observed in these disorders.

Stress can structurally remodel, in a reversible and adaptive manner, the neuronal connectivity in several brain regions, including the prefrontal cortex. This structural plasticity is dependent on a large variety of mediators, including those associated with the extracellular environment, such as cell-adhesion molecules (55). However, stressful experiences can also have long-term maladaptive consequences on neuronal circuitry. Daily life stressors are known to increase psychotic experiences and stress-related negative emotions (56). Severe life event stresses, through activation of the hypothalamic-pituitary-adrenal axis, induce a vital release of dopamine, the catabolism of which is known to generate ROS. Psychosocial stresses during brain development could result, when combined with GSH dysregulation, in an excess of ROS and oxidative damage, leading to progressive structural and functional connectopathy. Traumatic experiences during childhood thus enhance the risk for psychosis.

Taken together, excessive ROS production, generated during strong environmental insults, and particularly in at-risk individuals for redox dysregulation, will have a potent effect on fast-spiking cells bearing immature or abnormal PNNs. Given the pivotal role of PV cells and PNNs in regulating the onset and closure of brain plasticity (52, 57), oxidative stress may contribute to the slow emergence of psychoses by mistiming key windows of brain development. Our data provide a unique function and therapeutic insight presented by this specialized extracellular matrix structure in psychiatric disorders.

Materials and Methods

Animals. *Gclm* KO mice (36) were provided by Y. Chen (University of Colorado Denver). *Gclm* KO mice were backcrossed with C57BL/6J mice over >10 generations. *PV-Gclc* KO mice were obtained by crossing mice having *Gclc* gene flanked by *loxP* sites (*Gclc* floxed) (58) (provided by Y. Chen) with mice expressing Cre recombinase in PV cells (*PV-Cre* mice) (59) (S. Arber, University of Basel, Switzerland). *PV-Cre* mice were used as controls (*PV-Gclc* WT). Experiments were approved by and performed in accordance with the guidelines of the Veterinary Office of the Canton de Vaud in Switzerland and the Harvard Institutional Animal Care and Use Committee in the United States.

Induction of an Additional Oxidative Challenge. Additional oxidative stress was generated in regions richly innervated by dopaminergic neurons (i.e., the ACC) with the dopamine reuptake inhibitor GBR. GBR (BioTrend AG) was injected (s.c. 5 mg/kg) daily in *Gclm* KO and WT mice either from postnatal days P10 to P20 (preweaning) or from P80 to P90 (young adult). PBS was used for the control injection.

Surgery and Chondroitinase ABC Treatment. Intracortical injection of ChABC (from *Proteus vulgaris*, Sigma-Aldrich) was used to degrade PNNs in the ACC

of young adult (P90) *Gclm* KO mice. ChABC degrades chondroitin sulfate proteoglycans, which are a major component of the PNNs (32). Cortical injection of ChABC fully removed labeling by the lectin WFA, which binds PNNs without causing any inflammatory processes (56). Mice were anesthetized with ketamine/xylazine (73/11.6 mg/kg, i.p.). Isoflurane was used to keep the mice in a deep state of anesthesia throughout the surgical procedure. Bilateral craniotomy was performed (Bregma, ∼1.2; lateral, ∼0.25; depth, ∼1.25 mm) to inject 1 μL ChABC (50 U/mL; 0.1 μL/min; see ref. 60) into one ACC and 1 μL vehicle solution (PBS with 0.1% BSA) into the contralateral ACC. As analgesics, lidocaine (Wacker Chemie AG) was applied locally, and buprenorphine (Temgesic, Essex Chemie AG) was injected (0.1 mg /kg, s.c.) immediately after surgery. GBR treatment was initiated 4 d after the ChABC injection.

Immunohistochemistry and Stereological Quantification. Parvalbumin immunohistochemistry and stereological quantification of PV cells in the ACC were performed as described in detail in the *SI Materials and Methods*. The mean number of PV cells per unit volume in the ACC was compared between genotypes or treatments, using one-way ANOVA followed by post hoc Dunnett multiple comparisons.

Immunostaining, Confocal Microscopy, and Image Analysis. Immunofluorescence histochemistry for 8-oxo-dG, PV, calbindin, calretinin, and WFA-labeled PNNs was performed as described in the *SI Materials and Methods*. Quantification of 8-oxo-dG labeling and number of PV, calbindin, and calretinin immunoreactive cells or PV cells with WFA-labeled PNNs was done as described in *SI Materials and Methods*. General 8-oxo-dG labeling (mean fluorescence intensity in arbitrary units), number of PV cells, number of PV cells with WFA-labeled PNNs, and percentage of PV cells with WFA-labeled PNNs were compared between the two genotypes and treatments (when applied), using multivariate ANOVA followed by Dunnett tests. The number of PV, calbindin, and calretinin cells and the overall 8-oxo-dG labeling in ChABC-injected ACC and contralateral sham ACC in PBS- and GBR-treated mice were compared using multivariate ANOVA and pair-wise Dunnett tests. To analyze the relationship between PNN robustness and oxidative stress in PV cells, we used rank-transformed values of the number of WFA-labeled voxels around PV cells and the number of 8-oxo-dG–labeled voxels in PV cells (with Gaussian distribution) to calculate the Pearson correlation coefficient, and tested the significance. We used JMP8 Statistical Discovery Software (SAS Inc.) to plot the quantile density contours and linear regression.

Electrophysiology. Slices through the ACC were prepared on a vibroslicer in aerated artificial cerebrospinal fluid (ACF) (in mM: 252 sucrose, 3 KCl, 2 $MgSO_4$, 1.2 $CaCl_2$, 1.2 NaH_2PO_4, 24 $NaHCO_3$, and 10 glucose at pH 7.4) and maintained in interface chambers superfused with aerated ACF (in mM: 126 NaCl, 3 KCl, 1 $MgCl_2$, 1.2 $CaCl_2$, 1.2 NaH_2PO_4, 24 $NaHCO_3$, and 10 glucose at pH 7.4). Field potentials were recorded with ACF-filled electrodes (∼1 MΩ). Oscillations were induced with 50 μM carbachol, 0.8 μM kainic acid, and 1 μM quinpirole in 5 mM KCl-containing ACF. Signals were band pass-filtered at 0.3–1,000 Hz and digitized at 5 kHz. Once oscillations became stable, a 60-s recording was used for the power spectrum analysis, using the Welch method (IgorPro6, WaveMetrics). For each mouse, recordings were performed in both ACC along two to three consecutive slices. The power density of β and γ, which was calculated from the integral of the power spectrum within 13–28 and 30–60 Hz, respectively, and their peak frequencies were compared across genotypes, using independent sample *t* tests.

To study the effect of PNN degradation, we recorded and analyzed oscillations induced by coapplication of carbachol, kainic acid, and quinpirole in ACC that were previously injected with ChABC and compared with contralateral sham ACC. Recordings were performed bilaterally in three to four slices spanning the injection sites. After the recordings, each slice (400 μm thick) was then fixed with 40 g/L paraformaldehyde and recut into 40-μm frozen sections. Two noncontiguous sections for each 400-μm slice were used to check for WFA labeling and PV immunoreactivity. Only recordings from slices displaying little or no WFA labeling in the ChABC-injected ACC compared with the contralateral sham ACC were analyzed. This verification was done blindly before performing the electrophysiological analysis. The effects of ChABC and GBR treatment and their interaction on the power of oscillations were assessed using a multivariate analysis, with treatment (PBS vs. GBR) as the between-subject factor and with PNN status (ChABC-injected vs. sham-injected ACC) as the within-subject factor.

1. Sohal VS, Zhang F, Yizhar O, Deisseroth K (2009) Parvalbumin neurons and gamma rhythms enhance cortical circuit performance. *Nature* 459(7247):698–702.
2. Whittington MA, Cunningham MO, LeBeau FE, Racca C, Traub RD (2011) Multiple origins of the cortical γ rhythm. *Dev Neurobiol* 71(1):92–106.
3. Cabungcal JH, Steullet P, Kraftsik R, Cuenod M, Do KQ (2013) Early-life insults impair parvalbumin interneurons via oxidative stress: Reversal by N-acetylcysteine. *Biol Psychiatry* 73(6):574–582.
4. Behrens MM, et al. (2007) Ketamine-induced loss of phenotype of fast-spiking interneurons is mediated by NADPH-oxidase. *Science* 318(5856):1645–1647.
5. Powell SB, Sejnowski TJ, Behrens MM (2012) Behavioral and neurochemical consequences of cortical oxidative stress on parvalbumin-interneuron maturation in rodent models of schizophrenia. *Neuropharmacology* 62(3):1322–1331.
6. Schiavone S, et al. (2009) Involvement of NOX2 in the development of behavioral and pathologic alterations in isolated rats. *Biol Psychiatry* 66(4):384–392.
7. Grillo CA, et al. (2003) Region specific increases in oxidative stress and superoxide dismutase in the hippocampus of diabetic rats subjected to stress. *Neuroscience* 121(1):133–140.
8. Hu W, Zhang M, Czéh B, Flügge G, Zhang W (2010) Stress impairs GABAergic network function in the hippocampus by activating nongenomic glucocorticoid receptors and affecting the integrity of the parvalbumin-expressing neuronal network. *Neuropsychopharmacology* 35(8):1693–1707.
9. Lewis DA, Fish KN, Arion D, Gonzalez-Burgos G (2011) Perisomatic inhibition and cortical circuit dysfunction in schizophrenia. *Curr Opin Neurobiol* 21(6):866–872.
10. Torrey EF, et al. (2005) Neurochemical markers for schizophrenia, bipolar disorder, and major depression in postmortem brains. *Biol Psychiatry* 57(3):252–260.
11. Zhang ZJ, Reynolds GP (2002) A selective decrease in the relative density of parvalbumin-immunoreactive neurons in the hippocampus in schizophrenia. *Schizophr Res* 55(1-2):1–10.
12. Barr MS, et al. (2010) Evidence for excessive frontal evoked gamma oscillatory activity in schizophrenia during working memory. *Schizophr Res* 121(1-3):146–152.
13. Cho RY, Konecky RO, Carter CS (2006) Impairments in frontal cortical gamma synchrony and cognitive control in schizophrenia. *Proc Natl Acad Sci USA* 103(52):19878–19883.
14. Spencer KM, Niznikiewicz MA, Shenton ME, McCarley RW (2008) Sensory-evoked gamma oscillations in chronic schizophrenia. *Biol Psychiatry* 63(8):744–747.
15. Uhlhaas PJ, Singer W (2011) The development of neural synchrony and large-scale cortical networks during adolescence: Relevance for the pathophysiology of schizophrenia and neurodevelopmental hypothesis. *Schizophr Bull* 37(3):514–523.
16. Andreazza AC, et al. (2008) Oxidative stress markers in bipolar disorder: A meta-analysis. *J Affect Disord* 111(2-3):135–144.
17. Yao JK, Keshavan MS (2011) Antioxidants, redox signaling, and pathophysiology in schizophrenia: An integrative view. *Antioxid Redox Signal* 15(7):2011–2035.
18. Do KQ, et al. (2000) Schizophrenia: Glutathione deficit in cerebrospinal fluid and prefrontal cortex in vivo. *Eur J Neurosci* 12(10):3721–3728.
19. Gawryluk JW, Wang JF, Andreazza AC, Shao L, Young LT (2011) Decreased levels of glutathione, the major brain antioxidant, in post-mortem prefrontal cortex from patients with psychiatric disorders. *Int J Neuropsychopharmacol* 14(1):123–130.
20. Wang JF, Shao L, Sun X, Young LT (2009) Increased oxidative stress in the anterior cingulate cortex of subjects with bipolar disorder and schizophrenia. *Bipolar Disord* 11(5):523–529.
21. Gysin R, et al. (2007) Impaired glutathione synthesis in schizophrenia: Convergent genetic and functional evidence. *Proc Natl Acad Sci USA* 104(42):16621–16626.
22. Tosic M, et al. (2006) Schizophrenia and oxidative stress: Glutamate cysteine ligase modifier as a susceptibility gene. *Am J Hum Genet* 79(3):586–592.
23. Gokhale A, et al. (2012) Quantitative proteomic and genetic analyses of the schizophrenia susceptibility factor dysbindin identify novel roles of the biogenesis of lysosome-related organelles complex 1. *J Neurosci* 32(11):3697–3711.
24. Goldshmit Y, Erlich S, Pinkas-Kramarski R (2001) Neuregulin rescues PC12-ErbB4 cells from cell death induced by H(2)O(2). Regulation of reactive oxygen species levels by phosphatidylinositol 3-kinase. *J Biol Chem* 276(49):46379–46385.
25. Krishnan N, Dickman MB, Becker DF (2008) Proline modulates the intracellular redox environment and protects mammalian cells against oxidative stress. *Free Radic Biol Med* 44(4):671–681.
26. Otte DM, et al. (2011) N-acetyl cysteine treatment rescues cognitive deficits induced by mitochondrial dysfunction in G72/G30 transgenic mice. *Neuropsychopharmacology* 36(11):2233–2243.
27. Park YU, et al. (2010) Disrupted-in-schizophrenia 1 (DISC1) plays essential roles in mitochondria in collaboration with Mitofilin. *Proc Natl Acad Sci USA* 107(41):17785–17790.
28. Do KQ, Cabungcal JH, Frank A, Steullet P, Cuenod M (2009) Redox dysregulation, neurodevelopment, and schizophrenia. *Curr Opin Neurobiol* 19(2):220–230.
29. Kulak A, et al. (2013) Redox dysregulation in the pathophysiology of schizophrenia and bipolar disorder: Insights from animal models. *Antioxid Redox Signal* 18(12):1428–1443.
30. Giamanco KA, Morawski M, Matthews RT (2010) Perineuronal net formation and structure in aggrecan knockout mice. *Neuroscience* 170(4):1314–1327.
31. Carulli D, et al. (2010) Animals lacking link protein have attenuated perineuronal nets and persistent plasticity. *Brain* 133(Pt 8):2331–2347.
32. Kwok JC, Dick G, Wang D, Fawcett JW (2011) Extracellular matrix and perineuronal nets in CNS repair. *Dev Neurobiol* 71(11):1073–1089.
33. Sugiyama S, Prochiantz A, Hensch TK (2009) From brain formation to plasticity: Insights on Otx2 homeoprotein. *Dev Growth Differ* 51(3):369–377.
34. Morawski M, Brückner MK, Riederer P, Brückner G, Arendt T (2004) Perineuronal nets potentially protect against oxidative stress. *Exp Neurol* 188(2):309–315.
35. Suttkus A, Rohn S, Jäger C, Arendt T, Morawski M (2012) Neuroprotection against iron-induced cell death by perineuronal nets - an in vivo analysis of oxidative stress. *Am J Neurodegener Dis* 1(2):122–129.
36. Yang Y, et al. (2002) Initial characterization of the glutamate-cysteine ligase modifier subunit Gclm(-/-) knockout mouse. Novel model system for a severely compromised oxidative stress response. *J Biol Chem* 277(51):49446–49452.
37. Steullet P, et al. (2010) Redox dysregulation affects the ventral but not dorsal hippocampus: Impairment of parvalbumin neurons, gamma oscillations, and related behaviors. *J Neurosci* 30(7):2547–2558.
38. Härtig W, Brauer K, Bigl V, Brückner G (1994) Chondroitin sulfate proteoglycan-immunoreactivity of lectin-labeled perineuronal nets around parvalbumin-containing neurons. *Brain Res* 635(1-2):307–311.
39. Cadet JL, Brannock C (1998) Free radicals and the pathobiology of brain dopamine systems. *Neurochem Int* 32(2):117–131.
40. Rabinovic AD, Hastings TG (1998) Role of endogenous glutathione in the oxidation of dopamine. *J Neurochem* 71(5):2071–2078.
41. Feenstra MG, Vogel M, Botterblom MH, Joosten RN, de Bruin JP (2001) Dopamine and noradrenaline efflux in the rat prefrontal cortex after classical aversive conditioning to an auditory cue. *Eur J Neurosci* 13(5):1051–1054.
42. Lataster J, et al. (2011) Psychosocial stress is associated with in vivo dopamine release in human ventromedial prefrontal cortex: A positron emission tomography study using [¹⁸F]fallypride. *Neuroimage* 58(4):1081–1089.
43. Morawski M, et al. (2004) The binding of iron to perineuronal nets: A combined nuclear microscopy and Mössbauer study. *Hyperfine Interact* 159:285–291.
44. Campo GM, et al. (2004) Reduction of DNA fragmentation and hydroxyl radical production by hyaluronic acid and chondroitin-4-sulphate in iron plus ascorbate-induced oxidative stress in fibroblast cultures. *Free Radic Res* 38(6):601–611.
45. Cañas N, et al. (2007) Chondroitin sulfate protects SH-SY5Y cells from oxidative stress by inducing heme oxygenase-1 via phosphatidylinositol 3-kinase/Akt. *J Pharmacol Exp Ther* 323(3):946–953.
46. Pitts MW, et al. (2012) Deletion of selenoprotein P results in impaired function of parvalbumin interneurons and alterations in fear learning and sensorimotor gating. *Neuroscience* 208:58–68.
47. Rees MD, Hawkins CL, Davies MJ (2004) Hypochlorite and superoxide radicals can act synergistically to induce fragmentation of hyaluronan and chondroitin sulphates. *Biochem J* 381(Pt 1):175–184.
48. Zhang QG, et al. (2012) Critical role of NADPH oxidase in neuronal oxidative damage and microglia activation following traumatic brain injury. *PLoS ONE* 7(4):e34504.
49. Harris NG, Mironova YA, Hovda DA, Sutton RL (2010) Pericontusion axon sprouting is spatially and temporally consistent with a growth-permissive environment after traumatic brain injury. *J Neuropathol Exp Neurol* 69(2):139–154.
50. Pantazopoulos H, Woo TU, Lim MP, Lange N, Berretta S (2010) Extracellular matrix-glial abnormalities in the amygdala and entorhinal cortex of subjects diagnosed with schizophrenia. *Arch Gen Psychiatry* 67(2):155–166.
51. Kähler AK, et al. (2011) Candidate gene analysis of the human natural killer-1 carbohydrate pathway and perineuronal nets in schizophrenia: B3GAT2 is associated with disease risk and cortical surface area. *Biol Psychiatry* 69(1):90–96.
52. Beurdeley M, et al. (2012) Otx2 binding to perineuronal nets persistently regulates plasticity in the mature visual cortex. *J Neurosci* 32(27):9429–9437.
53. Miyata S, Komatsu Y, Yoshimura Y, Taya C, Kitagawa H (2012) Persistent cortical plasticity by upregulation of chondroitin 6-sulfation. *Nat Neurosci* 15(3):414–422, S1–S2.
54. Gandal MJ, Nesbitt AM, McCurdy RM, Alter MD (2012) Measuring the maturity of the fast-spiking interneuron transcriptional program in autism, schizophrenia, and bipolar disorder. *PLoS ONE* 7(8):e41215.
55. McEwen BS (2012) The ever-changing brain: Cellular and molecular mechanisms for the effects of stressful experiences. *Dev Neurobiol* 72(6):878–890.
56. Myin-Germeys I, Delespaul P, van Os J (2005) Behavioural sensitization to daily life stress in psychosis. *Psychol Med* 35(5):733–741.
57. Hensch TK (2005) Critical period plasticity in local cortical circuits. *Nat Rev Neurosci* 6(11):877–888.
58. Chen Y, et al. (2007) Hepatocyte-specific Gclc deletion leads to rapid onset of steatosis with mitochondrial injury and liver failure. *Hepatology* 45(5):1118–1128.
59. Hippenmeyer S, et al. (2005) A developmental switch in the response of DRG neurons to ETS transcription factor signaling. *PLoS Biol* 3(5):e159.
60. Pizzorusso T, et al. (2002) Reactivation of ocular dominance plasticity in the adult visual cortex. *Science* 298(5596):1248–1251.

NEUROSCIENCE